Multi-objective Evolutionary Optimization of Transonic Natural Laminar Flow Wing at High Reynolds Number

Shaojun Luo , Zhili Tang * , Yongbin Chen

Posted Date: 12 September 2024

doi: 10.20944/preprints202409.0973.v1

Keywords: Variable-fidelity hierarchical evolutionary optimization; Pareto non-dominated solutions; Transition predicition; Natural laminar flow wing; Shock wave control technology

 doi:10.20944/preprints202409.0973.v1

Article

Multi-Objective Evolutionary Optimization of Transonic Natural Laminar Flow Wing at High Reynolds Number

Shaojun Luo, Zhili Tang * and Yongbin Chen

College of Aerospace Engineering, Nanjing University of Aeronautics and Astronautics, Nanjing 210016, China
* Correspondence: tangzhili@nuaa.edu.cn

Abstract: Drag reduction by laminarization, an innovative technology in aerodynamics design, provides the possibility to improve significantly the aerodynamic performance of aircraft and remains to be one of the most promising and effective technologies. In this paper, the design method for transonic natural laminar flow wing at high Reynolds number is investigated in details and a new optimization model is established to solve conflicts between the increase of a laminar flow region and the shock wave strength at the trailing edge. In order to numerically handle this competitive situation efficiently, a two-objective hierarchical variable fidelity Pareto evolutionary optimization model based on search space contraction is proposed and implemented. Numerical experiments show that it can capture simultaneously a Pareto front of the two-objectives: a wave drag minimization and a laminar flow region maximization. The results also show that both wave drag and skin friction drag performances of non-dominated Pareto members can be significantly improved via the optimal laminar wing shape and shock wave control device. Nearly 40% of the laminar flow area on the wing surface is achieved at the Reynolds number of 10^7. It is concluded that the present hierarchical variable-fidelity multi-objective evolutionary optimization method is computationally efficient, and illustrate its potential for solving complex engineering design problems.

Keywords: variable-fidelity hierarchical evolutionary optimization; pareto non-dominated solutions; transition predicition; natural laminar flow wing; shock wave control technology

MSC: 68T20; 90C26

1. Introduction

The drag of modern long range civil airliners operating in transonic regime is mainly composed of frictional and lift-induced drag, accounting for about 55% and 35% of the total drag respectively[1]. According to the Breguet formula, it can be observed that three or four additional passengers would be carried for a 150-seat civil airplane with each count reduction ($\Delta C_D = 0.0001$) of drag when the flight distance remains constant. Therefore, it is very important to pursue the research on reducing the friction drag (mainly turbulent friction drag). Whereas, laminarization is one of the potential and effective turbulent drag reduction technologies in the future.

In recent years, many organizations and scholars have used optimization methods to carry out research on natural laminar flow (NLF) wing design. Lee and Jameson[2] carried out the research on NLF airfoil design with inverse design methods based on target pressure distribution, and generated three-dimensional (3D) wing shape for the drag reduction optimization using optimized airfoil profile. Amoignon et al.[3] considered the kinetic energy of the boundary layer as an objective function of the aircraft operating at transonic regimes, to delay the laminar-turbulent transition position with an optimization procedure. Hua et al. [4] designed supercritical NLF airfoil by inverse design method based on pressure distribution, and proposed the approach of using weak shock wave to form sufficient favorable pressure gradient for supercritical NLF airfoil design. Song, Zhu, et al.[5] coupled N_{TS}/N_{CF} transition prediction model based on linear stability theory with Reynolds averaged Navier-Stokes (RANS) solver as a flow transition prediction software, and carried out the research on drag reduction by laminar flow wing design. In reference[6], an optimization design method of supercritical natural

 doi:10.20944/preprints202409.0973.v1

laminar flow airfoil based on genetic algorithms (GAs) and computational fluid dynamics (CFD) is conducted, and the class shape transformation (CST) method is adopted as geometry parameterization method to carry out the optimization design of natural laminar wing based on the optimized airfoil.

It is very important to predict accurately the transition position for NLF wing design due to the procedure of transition from laminar to turbulence being complex. However, after more than half a century of theoretical and experimental research, the understanding of transition mechanism has been deepened and many boundary layer transition prediction methods have been developed. Among these methods, the e^N transition prediction method based on linear stability theory proposed by Smith[7], Stock and Ingen[8] has been widely used in aviation industry. After the e^N method was successfully applied in the case of two-dimensional boundary layer flow transition prediction, Arnal[9] and Cebeci[10] extended the e^N method to 3D problems. Stock and Haase[11] studied the mechanism of flow transition induced by flow direction instability and cross flow instability, and investigated flow transition prediction research by the method of solving RANS equations coupled with linear stability equations. Krumbein[12] used the linear parallel flow stability theory coupled with e^N method to predict the transition position. Meanwhile, he also carried out a research to ensure the value of empirical N at different flow conditions. Firstly, the estimated value is obtained by the Mack empirical formula, and then validated by experimental data. Song, Wu, et al.[13] coupled a N_{TS}/N_{CF} transition prediction model with a RANS solver to improve the accuracy of the solver. By solving the 3D stability equations, the integral amplification factor N_{TS} corresponding to Tollmien-Schlichting (T-S) wave is calculated by the e^N method, the integral amplification factor N_{CF} corresponding to cross-flow is calculated by a fixed β, and then the transition position is determined according to a threshold value.

The flow field around the aircraft with Navier-Stokes simulation is CPU time-consuming in aerodynamic shape design, this results in time-consuming evolution optimization of a complete aircraft based on flow simulation, making it difficult to perform 3D NLF shape design. Moreover, the initial guess point of many optimization methods is sensitive on the number of iterations. A proper initial design guess can significantly accelerate the optimization algorithm to find a global optimal solution much faster. Therefore, it can save CPU time to find the appropriate initial design point before starting simulation, the optimal initial point can be quickly found by using a variable-fidelity analysis model implemented in the aircraft design optimization[14]. A variable-fidelity model consists of both high-fidelity and low-fidelity model. The CPU time required when using a low-fidelity model is small, but its accuracy is poor, therefore, the evaluation of a large number of samples can be easily computed. On the other hand, the CPU time using high fidelity model is expensive and the accuracy is high, restricting to a small number of samples to be computed. The numerical performances of the variable-fidelity model are obtained alternatively by the low-fidelity model predicting the overall trend of the objective function while the high-fidelity model improves the accuracy of computerized results. In recent years, the CFD scientific community has proposed many new methods on variable-fidelity models successfully applied in practical projects. Han et al.[15] has carried out the research on aircraft aerodynamic shape optimization using variable-fidelity surrogate models. In order to reduce the number of high-fidelity simulations further, he used a three-level multi-fidelity model in aircraft design. His recent paper proposes a novel variable-fidelity optimization approach with application to aerodynamic design. Huang et al.[16] constructed an efficient multi-fidelity surrogate model based on two independent high and low fidelity samples. Their paper uses a larger quantity of low-fidelity information to enhance the accuracy of a surrogate of the high-fidelity model by modeling the correlation between high and low fidelity model, making the computational cost of the built surrogate model can be significantly reduced. In reference [17], Kriging based scaling function is introduced to better approximate the high-fidelity response on a global level. An adaptive hybrid method is also developed. This method combines the additive and multiplicative approaches such that the designer has not to determine the most suitable guess shape prior to optimization.

One of the main elements of this paper is to extend the variable-fidelity hierarchical evolutionary algorithms (EAs) into multi-objective optimization coupled with cooperative Game theory for the

 doi:10.20944/preprints202409.0973.v1

design of transonic NLF wing shape at high Reynolds number efficiently. First, a multi-objective optimization model for solving NLF shape design is proposed, and a shock wave control technology with trailing edge devices is selected. Then, an EAs coupled with a Pareto game is proposed for the optimization design of NLF shapes at transonic flight conditions. In order to improve optimization efficiency, a multi-island GAs coupled with a variable-fidelity hierarchical model and a search space contraction is proposed and implemented; then, non-dominated Pareto solutions of wing shapes with maximum laminar flow area and minimum weak shock wave intensity at the trailing edge are numerically obtained. From the analysis of results, the optimization efficiency of present hierarchical method is much better than the one obtained with a traditional GAs based on solely high fidelity flow analysis under the same accurate optimal solutions. This conclusion illustrates the potential of present variable-fidelity hierarchical optimization method proposed in this paper to be used in industrial environments.

2. Optimization Modeling of Transonic NLF Wing at High Reynolds Number

The transonic NLF wing design at high Reynolds number is to delay the transition by maintaining a long favorable pressure gradient region on the wing surface, so as to reduce the large skin friction drag caused by turbulence. The higher the Reynolds number in the optimal design of a transonic NLF wing, the more it is necessary to maintain a stronger and longer-range of favorable pressure gradient in the stream-wise direction. However, the stronger and longer the favorable pressure region means that the lower the pressure closer to the trailing edge. It is well known that the trailing edge is the stagnation point (its static pressure is the total pressure), so in transonic flow, when the flow recovers from very low pressure to the total pressure at stagnation point in a short distance, it will produce strong shock wave and then produce large wave drag. Therefore, the higher the Reynolds number, the stronger the shock wave near the trailing edge of the natural laminar wing, and the greater the wave drag. In other words, although the laminar flow design at high Reynolds number can reduce the friction drag, the transonic shock wave induced drag will increase accordingly. That is, the design of transonic laminar flow at high Reynolds number is faced with the contradiction between the realization of a stronger and longer favorable pressure gradient region and the increase of trailing edge shock intensity [18], and the higher the Reynolds number, the more prominent the contradiction between them.

2.1. Multi-Objective Optimization Model for Transonic NLF Wing Design

In view of the above analysis, the shock intensity taking place at the trailing edge should be controlled simultaneously during the design of laminar flow shape. In order to satisfy these two objectives simultaneously, the single-objective optimization design of a laminar flow shape is replaced by a two-objective design optimization problem for a simultaneous laminarization and a shock wave control at transonic flow conditions. The multi-objective optimization problem is defined as follows: (a) shape design optimization of the laminar flow region of a wing to delay the transition position; (b) optimizing additional shock control devices (SCB) to minimize the shock intensity.

According to (a) and (b) a transonic NLF shape optimization model is defined as follows in (1):

$$\begin{cases} \max\limits_{(wing\ shape)} \mathcal{J}_1 = S_{NLF} \\ \min\limits_{(SCB)} \mathcal{J}_2 = C_{Dw} \\ subject\ to: \\ \qquad C_L \geq C_{L0} \\ \qquad A_{Section} \geq A_{0,Section} \end{cases} \tag{1}$$

 doi:10.20944/preprints202409.0973.v1

In (1), S_{NLF} represents the laminar flow area on the wing surface, it is the sum of the laminar flow area on the upper (S_{upper}) and lower (S_{lower}) surfaces of the wing (i.e. $S_{NLF} = S_{upper} + S_{lower}$), C_{Dw} is wave drag coefficient which represents shock wave intensity of wing/airfoil shape at transonic regimes, C_{L0} represents the constraint value of lift coefficient, and $A_{0,Section}$ represents area constraint of the wing section. We have discussed this laminar flow design optimization model in detail in references[18,19] for two-dimensional NLF airfoil design, and explained in detail why we choose the two objectives of maximizing laminar flow region and minimizing wave drag as the optimization model, rather than minimizing total drag as the optimization model. Here, it is extended directly and used to the 3D NLF wing shape design.

2.2. Shock Wave Control Technology with Trailing Edge Devices

In transonic flight conditions, the flow starts at the leading edge of the airfoil, accelerates to become supersonic after passing through a series of expansion waves, and then remains supersonic until close to the trailing edge. Then a shock wave is generated at the rear edge due to the pressure recovery, while the flow changes from a supersonic to a subsonic regime. In order to control the strong shock wave on the wing surface, several active flow control methods are proposed in the past decade, such as air blowing/suction technology, vortex generator, oscillating plate, etc[20]. The trailing edge device (TED) is a mechanical control device installed at the trailing edge of an airfoil/wing, which is smaller than the traditional control rudder and usually only sized with a 4% or less of the chord length[21]. The TED contain a variety of control shapes as shown in Figure 1, among them the Gurney flap, the split flap and the divergent trailing edge (DTE) are the most usual ones. Gurney flap was first proposed by Liebeck[22] in 1978. Divergent trailing edge was proposed by Boyd and James[23] in 1985 and applied in flow control.

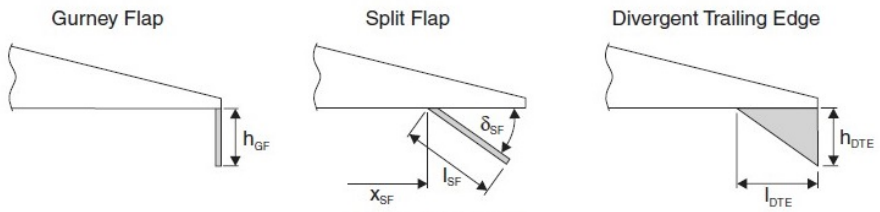

Figure 1. Shape and structure diagram of three trailing edge devices.

Usually, bump or TED techniques can be used to control the strong shock wave generated during the laminar flow wing design procedure[24,25]. However, when using the bump technology to control the shock wave at the trailing edge, there is a lack of robustness, which is a drawback on the control effect. In the other hand, the TED technology shows good aerodynamic robustness properties, and does not require lots of flow field grids to maintain both the efficiency and quality in the numerical optimization procedure of NLF wing shape design. When the TED is installed, the pressure does not need to be restored to the total pressure value at the rear stagnation point, and the shock wave strength is significantly reduced accordingly, while the wave drag is reduced compared to that of the baseline shape. A two-dimensional DTE device used to verify and analyze the effect of shock wave control on the airfoil surface has been demonstrated in[26]. Here, it is extended directly and used to the wave drag control in the design of 3D NLF wing.

3. Multi-Objective Hierarchical Variable Fidelity Pareto Evolutionary Optimization Algorithm for Transonic NLF Wing Design at High Reynolds Number

In the optimization design of NLF wing, it is necessary to accurately solve the 3D flow equations including transition model. However, it is different from the two-dimensional natural laminar flow shape design problem we solved previously [19], solving high-resolution 3D flow equations on fine meshes requires a lot of CPU time, which makes the actual shape optimization very difficult. Inspired by the multi-grid algorithms for the PDEs, we proposed the hierarchical optimization algorithms based

 doi:10.20944/preprints202409.0973.v1

on variable fidelity analysis in[27]. Here it will be extended to multi-objective shape optimization coupled with cooperative Pareto game, search space contraction as well as population size reduction, and used to solve the optimization design problem of NLF wing efficiently in this paper.

3.1. Multi-Objective Evolutionary Algorithms Coupled with a Pareto Game

There are several approaches to solve multi-objective optimization problems with genetic algorithms (GAs): i) aggregate objectives functions with a priori chosen weights, and then run an optimization design procedure with GAs; ii) non-dominated Pareto game solutions with multi-objective genetic algorithms; iii) GAs coupled with competitive Nash games [28]; iv) GAs coupled with hierarchical Stackelberg games [29]. Using weighted objective function to solve multi-objective optimization problem has many shortcomings, such as losing information or the difficulty to define a priori the weights of objective functions. In 1985, Schaffer was a pioneer with multi-objectives in proposing a genetic algorithm to solve a multi-objective problem using a vector evolutionary genetic algorithm (VEGA) software [30], which is biased towards the extreme value of each objective but does not require weights. In 1989, Goldberg proposed cooperative solutions based on Pareto ranking and sharing [31], which allow to capture the non-dominated solutions of a multi-objective problem spread over the whole Pareto front. Then the Pareto strategy coupled with evolutionary algorithms became the well known but expensive method for solving multi objective/multi disciplinary optimization problems.

Let N be the number of players, x be the vector of decision variables, the variable x belongs to a nonempty, closed and convex set $x \in X \subseteq R^n$, and normally $n \geq N$. Let $\mathcal{J}_\nu : R^n \mapsto R$ be the νth players payoff function. Let us define now the following cooperative optimization problem (2) [18]

$$min\ \mathcal{J}_\nu(x),\ \nu = 1, \cdots, N \tag{2}$$

Then introducing the definition of Pareto equilibrium: a solution x^1 is said to be dominating to another solution x^2 when

$$\forall\ \nu \in [1, N], \quad \mathcal{J}_\nu(x^1) \leq \mathcal{J}_\nu(x^2) \tag{3}$$

exists at least on ν such that $\mathcal{J}_\nu(x^1) < \mathcal{J}_\nu(x^2)$. The non-dominated solutions constitute the so called optimal Pareto front.

Then a usual approach to represent the solution of a multi-objective problem uses the concept of Pareto optimality or non-dominated individuals. Figure 2 shows the Pareto optimality concept for a problem with two cooperative objectives. Solutions to a given multi-objective problem belong to the optimal set, identified with a cooperative Pareto game which computes all the non-dominated solutions. This Pareto-GAs spans the complete range of compromised designs corresponding to the minimization of the two objectives. Most real life problems involve a number of non-separable objectives for which there is no unique optimum, but a set of trade-off individuals known as Pareto optimal (or non-dominated) solutions. The Pareto optimality principle is used when a solution to a multi-objective problem is considered Pareto optimal if there are no other solutions that better satisfy all the objectives simultaneously. The aim of this multi-objective optimization is then to provide the designer with a set of Pareto optimal solutions representing trade-offs among the multiple objectives.

 doi:10.20944/preprints202409.0973.v1

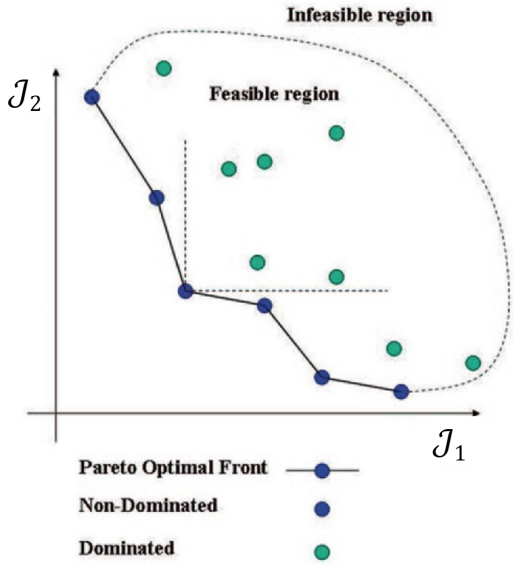

Figure 2. A schematic diagram to locate non-dominated Pareto front solutions.

3.2. Implementation of Multi-Objective Hierarchical Variable Fidelity Evolutionary Optimization for Transonic NLF Wing Design

Here, the above multi-objective Pareto evolutionary algorithm will be combined with variable fidelity analysis to solve the NLF wing shape design optimization. Three variable fidelity flow analysis models are used in this section. The low-fidelity flow analysis model is the potential flow equation with boundary layer correction, the medium-fidelity flow model is the Euler equations with boundary layer correction, and the high fidelity flow model is RANS equations. The reason why the viscous/inviscid iterative method is used in the optimization with low-fidelity flow analysis is that the NLF design is aimed at the attached flow, the inviscid and viscous iteration with additional boundary layer correction can not only obtain more accurate velocity profiles within the boundary layer, but also require less grids and much less CPU time than that of the RANS equation when obtaining the same accurate pressure distribution. It is well known that the slight saving of the flow calculation in aerodynamic shape design will significantly improve the computational efficiency of the actual engineering optimization problems. The transition prediction method used in the optimizations with above three flow fidelity analysis is an e^N method based on linear stability theory. In this section, many new techniques are introduced into the traditional variable fidelity optimization methods, such as search space contraction, reducing the number of design variables as well as population size reduction. The design procedure of the present multi-objective variable-fidelity hierarchical evolutionary optimization method coupled with a Pareto game for NLF wing design is defined as follows:

- *Optimization with low-fidelity flow analysis based on potential flow equation and boundary layer correction.* The multi-objective evolutionary optimization coupled with Pareto cooperative game starts from the design based on potential flow equation with boundary layer correction. Since the fitness analysis of individuals is based on the very efficient and inexpensive potential flow equation solving, it can be implemented on large search space with huge populations and sufficient evolutionary generations to guarantee sufficient convergence.
- *Transition from optimization with low fidelity model to optimization with medium fidelity model.* First of all, the search space is shrunk based on the well converged optimization results with low fidelity potential model. The reduced search interval is the largest aggregation subset of all design variables of the optimization result with low fidelity model. Then select the typical individuals by using niching technology from the previous converged optimal Pareto front to construct the new smaller initial population for optimization with medium fidelity Euler model. Finally, for those variables that have converged completely in the low-level optimization with low fidelity

Preprints.org (www.preprints.org) | NOT PEER-REVIEWED | Posted: 12 September 2024 doi:10.20944/preprints202409.0973.v1

analysis and are no longer sensitive to the cost function of the optimization with medium fidelity model, these variables can be frozen in the subsequent medium-level optimization to reduce the number of design variables.

- *Optimization with medium-fidelity flow analysis based on Euler equation and boundary layer correction.* Performing multi-objective evolutionary optimization again on the smaller population size and smaller search space with Euler solver addition to boundary layer correction, and the set of non-dominant solutions on the converged Pareto front is obtained after proper generation of evolutionary optimization.
- *Transition from optimization with medium fidelity model to optimization with high fidelity model.* This process is similar to the second step, which is to shrunk the search space, freeze converged or insensitive design variables, reduce the population size, and select the initial individuals for the next step of optimization.
- *Optimization with high-fidelity flow analysis based on RANS solver with second order numerical scheme.* Continue the multi-objective evolutionary optimization process on small population and small search space with RANS solver. In this step, only a few design variables that are still sensitive to the laminar flow region are optimized, such as the geometric shape near the leading edge. Therefore, the number of design variables is greatly reduced, and the population size is correspondingly greatly reduced. Although the evolutionary algorithm in high-level optimization needs to solve the RANS equation repeatedly, which consumes a lot of computing time, it only needs a few evolutionary generations in a small population and a small search space to get the final converged non-dominant Pareto solutions. Therefore, the total calculation times of RANS equation are limited, and the calculation time consumed in this high-level optimization will be greatly reduced.

The detailed process of the above algorithm is shown in following Figure 3. On the whole, the algorithm is a multi-objective evolutionary algorithms (MOEAs) based on variable fidelity analysis from low to high in a series of shrinking search interval and population size. In order to further improve the optimization efficiency, a multi-island parallel strategy is embedded, and the number of islands is also decreasing as the population size shrinks.

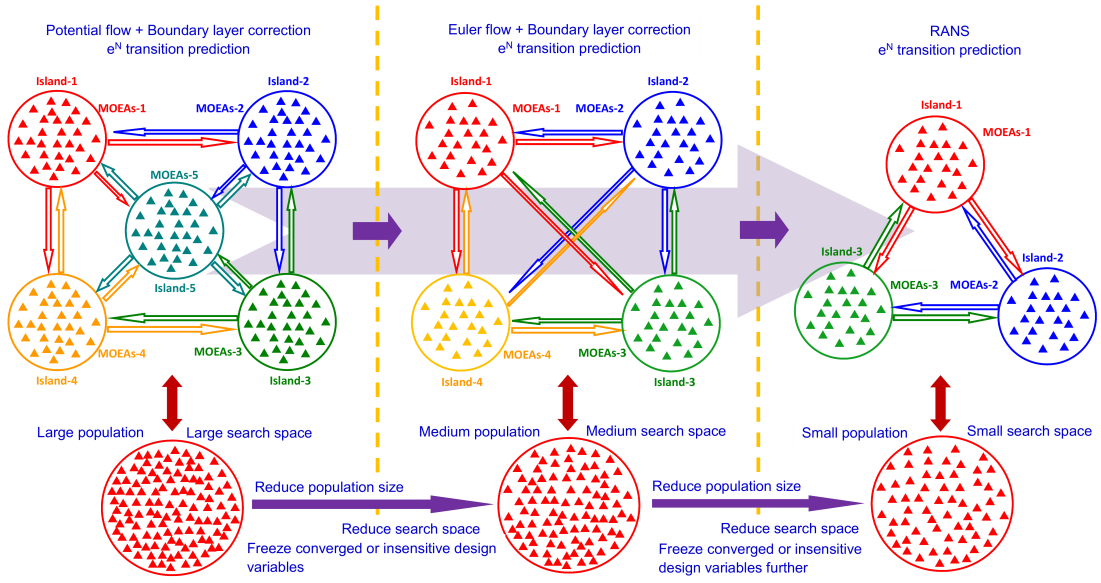

Figure 3. Schematic diagram of three-layer variable fidelity multi-objective Pareto evolutionary optimization algorithm for NLF shape design optimization.

3.3. Flow Field Analysis and Transition Prediction Methods Based on Variable-Fidelity Flow Analysis

In NLF wing shape dsign, a cheap 3D transition prediction tool is needed[32]. Among the different transition prediction tools, the e^N method based on linear stability theory is still an effective

 doi:10.20944/preprints202409.0973.v1

and fast prediction method. Linear stability theory is a transition prediction method based on small perturbation theory. By simulating the evolution of small perturbations in the flow field, it can be observed whether the perturbation increases or decreases with time to determine whether the flow transition occurs. If the disturbance decays, the flow is assumed to be laminar while if the disturbance amplitude increases along the flow direction, then the flow will transit into turbulence. Therefore, based on a variable-fidelity flow analysis and the linear stability theory, a variable-fidelity transition prediction method is then implemented in 3D NLF wing design. A detailed implementation procedure is described as follows:

- *Flow field analysis and transition prediction based on low-fidelity potential flow solver.* (a) For each given individual in the evolutionary algorithm, that is, it corresponds to a wing shape with TED. First, the potential flow equation is solved to obtain the velocity distribution on the wing surface. (b) From the velocity distribution, the boundary layer parameters, including the velocity profile distribution, the displacement thickness and the momentum loss thickness can be obtained by the solution of the boundary layer equations. The linear stability equations are solved based on the velocity profile and Reynolds number in the boundary layer. The transition location of the flow is obtained by using e^N method. Both the boundary layer equations and the linear stability equations are solved iteratively until the computation captures the stable transition position. New parameters such as the displacement thickness and the momentum loss thickness of the boundary layer can be then obtained. (c) Based on the displacement thickness of the boundary layer and the flow transition position, the transition position of the new shape with added displacement thickness is solved again, until reaching convergence of the boundary layer displacement thickness and transition position, the transition line of wing surface is finally obtained by a low-fidelity potential flow model. Thus, the laminar flow area S_{NLF} on the wing surface and the aerodynamic performance parameters of the wing, such as lift coefficient and wave drag coefficient, are obtained.
- *Flow field analysis and transition prediction based on medium-fidelity Euler solver.* This is similar to the previous step, which only needs to replace the calculation of potential flow equation with that of the Euler equations.
- *Flow field analysis and transition prediction based on high-fidelity RANS solver.* For a given wing with trailing edge shock control device, the corresponding aerodynamic characteristics, such as lift and/or drag coefficient, are obtained by solving the RANS equation. Then, according to the velocity distribution on outer edge of boundary layer provided by RANS equation, the 3D boundary layer equations is solved to obtain the accurate velocity profiles within boundary layer. Then the linear stability equation is solved and the transition position is predicted with e^N method. Repeat the iterative process between the boundary layer equation and the stability equation until the stable laminar flow area S_{NLF} on the wing surface is obtained.

The above viscous/inviscid coupled flow analysis can usually converge in two iterations, while the boundary layer flow analysis coupled with linear stability transition prediction can converge in four sub-iterations. The Euler and RANS flow equations are solved based on the implicit finite volume method on a multi-block hybrid grid. The inviscid flux is calculated by using the third-order ROE scheme, and the viscous momentum flux and heat flux are calculated by using the second-order central difference scheme. The S-A turbulent model with compressibility correction is used in the calculation of the RANS equations, and the convection term in the turbulence model is approximated by the second-order upwind scheme. The success of its application in NLF shape design has been verified in papers [18,19].

4. Multi-Objective Hierarchical Optimization Design of a NLF Wing Operating at Transonic Regime with a Variable-Fidelity Method

A straightforward conclusion from[18,19] shows that the laminarization of wing surface takes place with the delay of transition position, but increases the shock induced drag. Therefore, it is

 doi:10.20944/preprints202409.0973.v1

necessary to control simultaneously the shock intensity at the trailing edge of wing shape. A two-objective optimization model for laminarization design and shock wave control is introduced in section 2.1. In this section, a hierarchical variable-fidelity evolutionary optimization algorithm coupled with a cooperative Pareto game is used to optimize the wing shape in maximizing the laminar flow region and in minimizing the shock induced drag as the two optimization objectives at the following flight conditions: Mach number 0.735, angle of attack 2.0 degree and Reynolds number 9.128×10^6.

4.1. Definition of the NLF Wing Shape Optimization Problem Operating at Transonic Regime

During the wing shape optimization procedure, the lift coefficient and the contain area of the wing section are constrained, and a DTE is used for controlling the shock wave intensity. Considering the actual constraints and their numerical implementations in the optimization process, the multi-objective optimization model introduced in (1) including lift constraints is rewritten as follows:

$$\begin{cases} \max\limits_{(Wing,DTE)} \mathcal{J}_1 = (S_{upper} + S_{lower})(1 + \beta(C_L - C_{L0})/C_{L0}) \\ \min\limits_{(Wing,DTE)} \mathcal{J}_2 = C_{Dw}(1 - \beta(C_L - C_{L0})/C_{L0}) \\ where \;\; \beta = 0, when \;\; C_L \geq C_{L0}, \;\; otherwise \;\; \beta = 1. \end{cases} \tag{4}$$

where, S_{upper} and S_{lower} represent the laminar flow areas on the upper and the lower surfaces of the wing respectively, C_{Dw} the shock wave induced drag coefficient of the wing, x_{len} and x_{hei} the length and the height of the DTE. The planform shape and parameterization of the wing are shown in the Figure 4, and the leading edge sweep angle is 10^0. The whole wing is composed of eight control sections. The shape of each section is controlled by the CST parameterization constructed by the Bernstein polynomials of order 4. Each section has 12 control parameters (10 are from CST parameterization and 2 are from TED), and each parameter and its corresponding initial variation range are shown in the Table 1, where parameters marked with superscript (e.g. $\beta^{'}$, $b_1^{'}$, $b_2^{'}$ and $b_3^{'}$.) are lower surface parameters. So there are 96 control parameters (i.e. design variables) at most for the whole wing shape optimization.

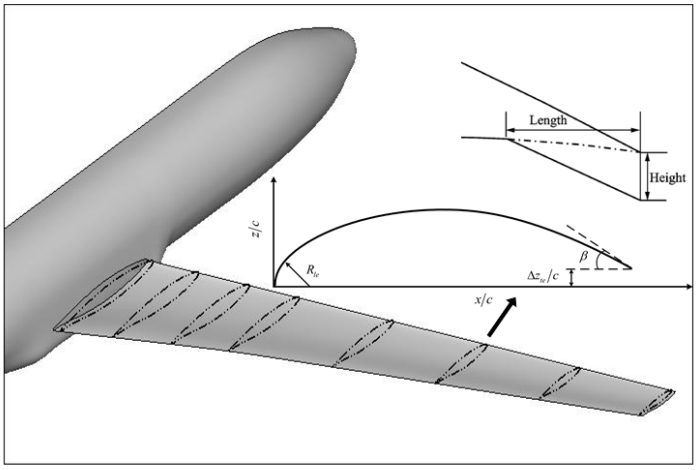

Figure 4. Wing planform shape and control sections.

 doi:10.20944/preprints202409.0973.v1

Table 1. Design variables of the wing sections and the corresponding search space of optimization with lower-fidelity flow solver.

Variables	Search space	Variables	Search space
R_{LE}/c	[0.005, 0.0075]	b_2/c	[0.10, 0.25]
β (rad)	[0.14, 0.28]	b_3/c	[0.10, 0.30]
$\beta^{'}$ (rad)	[0.00, 0.14]	$b_1^{'}/c$	[0.05, 0.20]
$\Delta Z_{TE}/c$	[-0.005, 0.005]	$b_2^{'}/c$	[0.05, 0.25]
b_1/c	[0.05, 0.20]	$b_3^{'}/c$	[0.10, 0.25]
x_{len}/c	[0.96, 0.975]	x_{hei}/c	[0.085, 0.105]

4.2. Numerical Implementation of NLF Wing Shape Optimization with Multi-Objective Hierarchical Variable Fidelity Evolutionary Method

In order to accelerate convergence and improve the efficiency of optimization, a variable-fidelity hierarchical optimization method introduced in section 3 is used to solve the multi-objective problem (4). During the low-fidelity optimization stage, eight sections are used to set up the wing geometry model, and fourth-order Bernstein polynomials are used in CST parameterization to build each section. Therefore the total number of design variables in the optimization is 96. Since the computational grid of the potential flow equation is very sparse (the overall structural grid surrounding the wing-fuselage combination shown in Figure 4, with a total of $0.3M$ grids.) and the solution time is very short, a large population size can be used. Here, the population size of the GA-optimizer in each generation is 1000. So we specify five islands for parallel optimization through individual migration in the multi-island parallel MOEAs shown in Figure 3. The optimization at this stage took 355 hours of CPU time, and the convergent result was obtained after 80 generations of evolution.

Remove the variables that have converged in the optimization with low-fidelity flow model and the variables that are not sensitive to medium-fidelity flow model. At this time, the parameters of the wing root and tip sections have converged and no longer evolved, and only the six design variables (R_{LE}, b_1, b_3, $b_1^{'}$, x_{len}, x_{hei}) in each of the middle six sections still sensitively affect the changes of the laminar flow region. So there are only 36 design variables at this medium-fidelity flow analysis based optimization, and the population size in each generation reduced to 400 instead of still maintaining the 1000 in the previous optimization. The search space for these 36 design variables is reduced according to the method described in section 3.2. Then 400 optimal representative individuals are selected from the previous converged Pareto front as the initial population for the optimization with medium-fidelity flow analysis. At this point in the multi-island parallel MOEAs algorithm in the smaller population, only four islands are sufficient as shown in Figure 3. After 20 generations of evolution, convergent results have been obtained. Although the population size and evolutionary generations at this stage are significantly reduced compared to that of in the previous optimization, it still took 400 hours of CPU time to converge, which is equivalent to the CPU cost in the optimization with low-fidelity model. This is because the computational cost of Euler equations is much greater than that of potential flow equation. In addition, the number of mesh cells for solving Euler equation is also more than that for solving potential flow equation.

On the basis of the optimal convergence solution with the medium-fidelity flow analysis, the optimization is further transformed into the optimization based on the high-fidelity RANS flow analysis. According to the sensitivity analysis results of transition position with respect to shape perturbation in NLF shape design optimization [33], we found that at this time, only design variables (R_{LE}, b_1) on each of six middle sections still have weak sensitivity. So now there are only 12 design variables left. The population size is taken as 90, and is divided into three islands for parallel optimization as shown in Figure 3. The reduction of search space and the selection of initial population are as the same as the previous ones. After 10 generations of parallel MOEAs optimization, the Pareto front converges, and it takes 62 hours of CPU time.

 doi:10.20944/preprints202409.0973.v1

The randomized crossover and mutation probability values are 0.8 and 0.1 respectively both in the low-fidelity based optimization and the high-fidelity based optimization stages, and the deterministic selection operator is based on best evaluated wing candidates. In order to compare the computational efficiency of the present multi-objective hierarchical optimization method based on variable fidelity flow analysis in solving NLF wing optimization, we also carried out the optimization directly based on RANS flow analysis, and found that the computational efficiency for such a complex engineering optimization problem was improved by nearly 10 times. Table 2 shows the CPU-time required to obtain converged solutions with a variable-fidelity hierarchical optimization method and an usual evolutionary optimization method without using variable-fidelity analysis. A converged solution of the $3D$ wing design problem is obtained with a variable-fidelity model hierarchical optimization method requiring 817 (i.e. $355 + 400 + 62$.) hours of CPU-time, which is much less compared with the one needed by an usual simple genetic algorithms (e.g. 6800 hours of optimization with RANS analysis only). Therefore, the variable-fidelity model based hierarchical optimization method implemented numerically in this paper is efficient and can be used as a design numerical tool for maximizing the laminar flow wing region in the refined parameter optimization stage of an aircraft design.

Table 2. Statistics of CPU-time cost for achieving the multi-objective optimization of a laminar flow wing design.

	With VFFA			**Without VFFA**
	low-fidelity	**Medium-fidelity**	**High-Fidelity**	**RANS solver**
Variables	96	36	12	96
Population	1000	400	90	1000
Islands	5	4	3	–
Generations	80	20	10	100
CPU cost (h)	355	400	62	6800

NOTE: VFFA means variable-fidelity flow analysis.

4.3. Optimization Results and Analysis of a Transonic NLF Wing

Figure 5 shows Pareto solutions for multi-objective problems (4) using the variable-fidelity model. It can be observed that the Pareto front is captured after a not expensive convergence of the optimization with the low-fidelity model. Then selecting the good representative individuals of the well converged optimization solution based on low-fidelity model as initial population guess for the optimization based on the high-fidelity model, the final converged Pareto solutions are captured simultaneously after achieving the high fidelity optimization convergence. It can be observed that the final optimized Pareto front obtained with the high-fidelity model is evidently shifted to the right of that with the low-fidelity model, which also indicates the improvement of the aerodynamic performances of the Pareto wings members. The set of non-dominated solutions on the Pareto front are tradeoffs of aerodynamic performances of wings and shock drag solutions at the trailing edge of the optimized wing. The laminar region of the wing increases with the delay of the transition line position on the wing surface. From a detailed analysis of results, it is concluded that the aerodynamic characteristic of laminar flow and shock intensity of wings corresponding to the Pareto front are improved simultaneously compared with the initial baseline shape, i.e. the shock wave drag intensity is effectively controlled and reduced while the laminar flow area on the wing surface increases.

 doi:10.20944/preprints202409.0973.v1

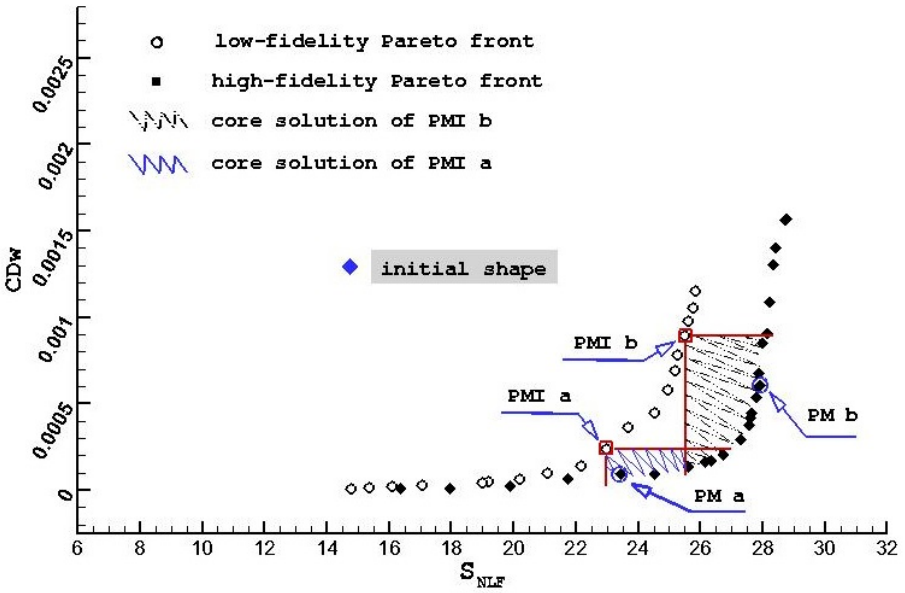

Figure 5. Two-objective Pareto front solutions for a NLF wing design.

According to the concept of a Pareto front with its non-dominated solution, an optimized Pareto member solution based on high fidelity model (namely *PMa*) is located below the low fidelity solution domain of *PMIa*, as shown on Figure 5. Therefore, the aerodynamic performances of the wing geometry corresponding to *PMa* is better than that of the wing geometry corresponding to *PMIa*. Similarly, the aerodynamic performances of wing geometry corresponding to *PMb* is better than that of wing shape corresponding to *PMIb*. The corresponding *PMa* and *PMb* wings have the same level of non-dominance sorting, therefore the Pareto front solutions including *PMa* and *PMb* are better in terms of drag values than the Pareto front solutions on which *PMIa* and *PMIb* are located. It is easily concluded that the aerodynamic performances of wing shapes obtained by a high-fidelity model are significantly improved compared to those obtained by optimization with a low-fidelity model.

Table 3 shows the comparison of aerodynamic performances for different wing shapes obtained by a low-fidelity model based optimization and a high-fidelity model based optimization with that of initial baseline wing shape. Analyzing the aerodynamic performance of different wing shapes, it can be concluded that the aerodynamic performance of new designed wing shapes has been significantly improved even after performing a low-fidelity model based optimization. The laminar flow area ratio on the upper surface of the baseline wing is 4.62%, while these values corresponding to the Pareto members *PMIa* and *PMIb* obtained by the low-fidelity model based optimization are increased to 26.4% and 33.67% respectively; the shock wave induced drag coefficient are 0.00024 and 0.00089, respectively, which are much less compared to the 0.00129 of the baseline wing shape. Furthermore, relying on the converged solutions based on the low-fidelity model, the number of design variables can be reduced, and it can continue to perform laminar wing optimization with high fidelity models based on it. Then, with this model, the laminar flow area on the wing surface is remotely expanded. The proportion of laminar flow regions on wings corresponding to Pareto members *PMa* and *PMb* located on the Pareto front captured with the high-fidelity model based optimization reach 28.22% and 38.9% respectively of the total wing area, while the skin friction drag coefficient on the wing surface is further reduced to 0.00441 and 0.00416 respectively. Meanwhile, the shock intensity at the trailing edge is effectively controlled, the corresponding shock wave induced drag coefficient values are 0.0001 and 0.0006 respectively, which are smaller than the value 0.00129 of the baseline wing shape. Finally the total drag coefficient is reduced from 0.01598 (the value of the baseline wing) to 0.01297 and 0.01350 respectively. It is concluded that the aerodynamic characteristics of the optimized wing shape

 doi:10.20944/preprints202409.0973.v1

configurations are significantly improved compared to the baseline wing shape, and it is numerically checked with these results that the laminar flow optimization model introduced and implemented in this paper is effective.

Table 3. Comparison of aerodynamic performance for different wing shapes.

	Initial shape	**low-fidelity solutions**		**high-fidelity solutions**	
		PMI a	**PMI b**	**PM a**	**PM b**
C_L	0.520	0.518	0.517	0.520	0.521
C_D	0.01598	0.01367	0.01368	0.01297	0.01350
$C_{D_{fU}}$	0.00283	0.00252	0.00226	0.00250	0.00225
$C_{D_{fL}}$	0.00220	0.00199	0.00198	0.00191	0.00191
C_{Dw}	0.00129	0.00024	0.00089	0.0001	0.0006
S_{upper}	1.7803	10.1645	12.9620	10.8646	14.9947
S_{lower}	12.9374	12.8213	12.5380	12.5583	12.9998

NOTE: C_L = Lift coefficient, C_D = Drag coefficient, $C_{D_{fU}}$ = Friction coefficient on upper surface of wing, $C_{D_{fL}}$ = Friction coefficient on lower surface of wing, C_{Dw} = Wave drag coefficient, S_{upper} = Area of laminar flow region on upper surface of wing (m^2), S_{lower} = Area of laminar flow region on lower surface of wing (m^2).

On Figures 6–8 are shown the pressure coefficients contours of the baseline wing shape and selected wing shape solutions corresponding to PMa and PMb members located on the converged Pareto front. Concerning the pressure coefficient distribution on the baseline wing surface, it can be observed that the flow near the root surface decelerates from the leading edge, and the instability is aggravated by the adverse pressure gradient, favoring an early transition of the flow to a turbulent regime. Although the tip sections of the wing maintains a large range of the flow direction which is favorable to a pressure gradient, the spanwise direction at tip sections has a strong adverse pressure gradient. Hence, the strong cross-flow instability triggers the flow transition and turns its regime to turbulence. Therefore, the flow on the upper surface of the initial wing shape is turbulent, and the skin friction drag coefficient is large. However, the optimized wing surface maintaining a wide range of flow-direction favorable pressure gradient while the pressure gradient in the spanwise direction is small, the transition on wing surface due to the flow direction and the spanwise direction instability is consequently delayed. On Figure 9–12 are presented laminar and turbulent flow regions on the upper and lower surfaces of the optimized wings corresponding to PMa and PMb members located on final Pareto front respectively, as well as transition line positions of the wing shapes obtained by the low-fidelity optimization ($PMIa$ and $PMIb$ members). It is observed that the laminar flow area on the wing surfaces increases greatly after a low-fidelity based optimization stage followed by high-fidelity stage optimization. The laminar flow area in the middle span-wise part on the optimized wing shape based on high-fidelity model is remotely expanded when compared with that of optimized wing shape based on low-fidelity model.

 doi:10.20944/preprints202409.0973.v1

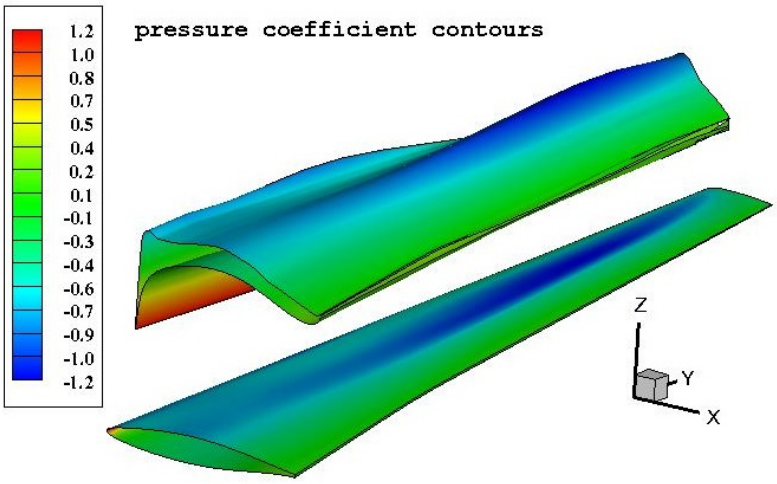

Figure 6. Pressure coefficient distribution contours on an initial wing shape.

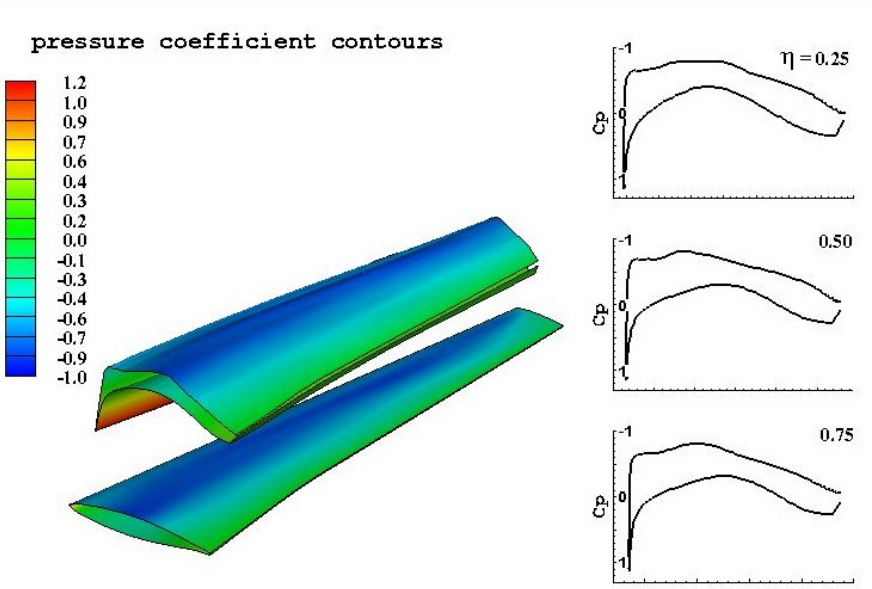

Figure 7. Distribution of pressure coefficient contours on an optimized wing corresponding to the Pareto member PM a solution.

 doi:10.20944/preprints202409.0973.v1

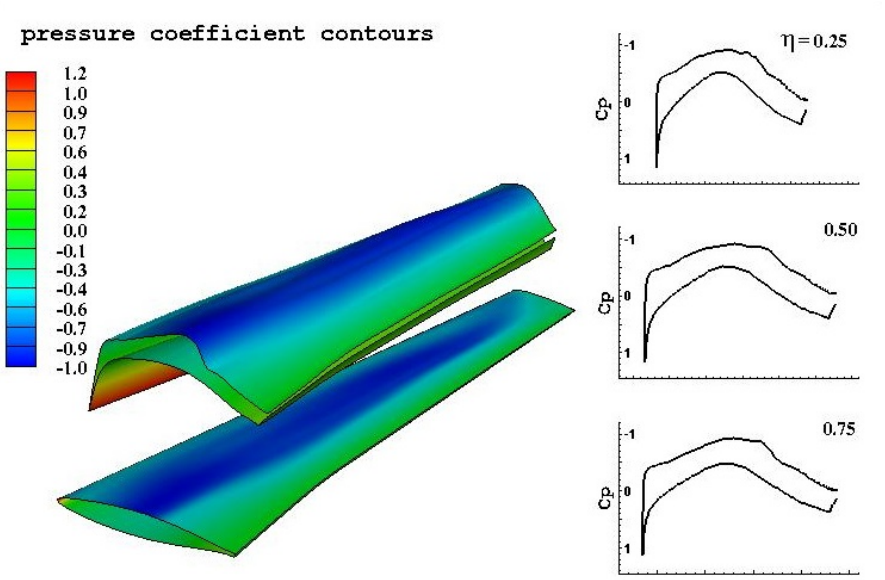

Figure 8. Distribution of pressure coefficient contours on an optimized wing corresponding to the Pareto member PM b solution.

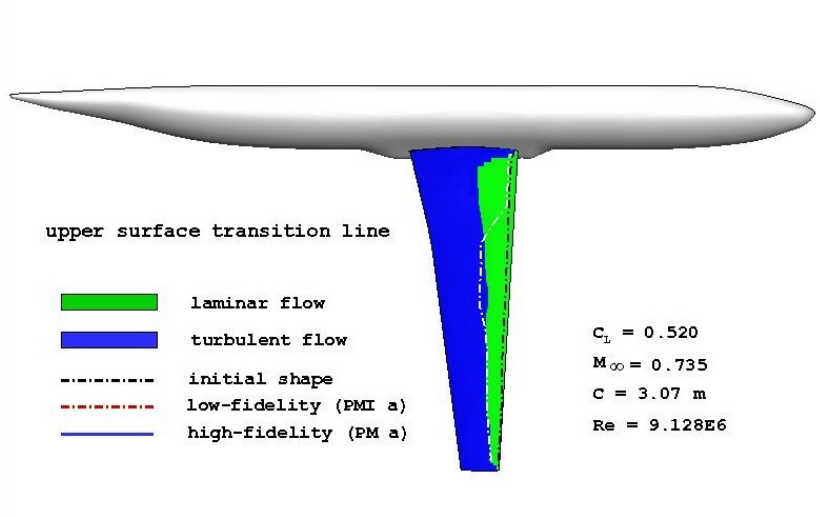

Figure 9. Transition lines on the upper surface of the baseline and optimized wing shape corresponding to *PMIa* and *PMa* solutions.

 doi:10.20944/preprints202409.0973.v1

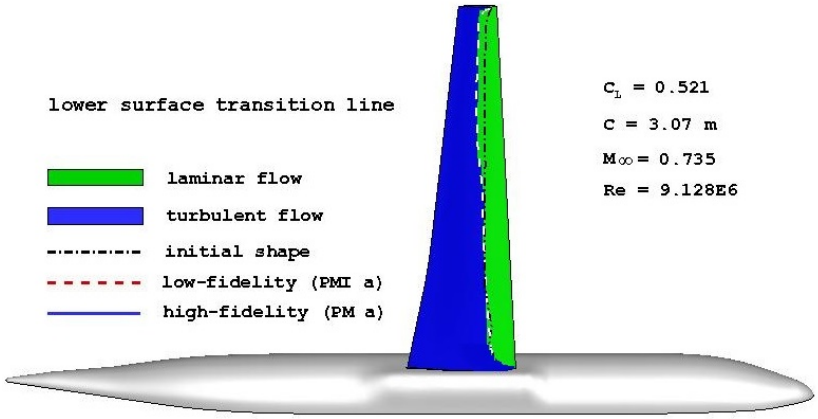

Figure 10. Transition lines on the lower surface of the baseline and optimized wing shape corresponding to *PMIa* and *PMa*.

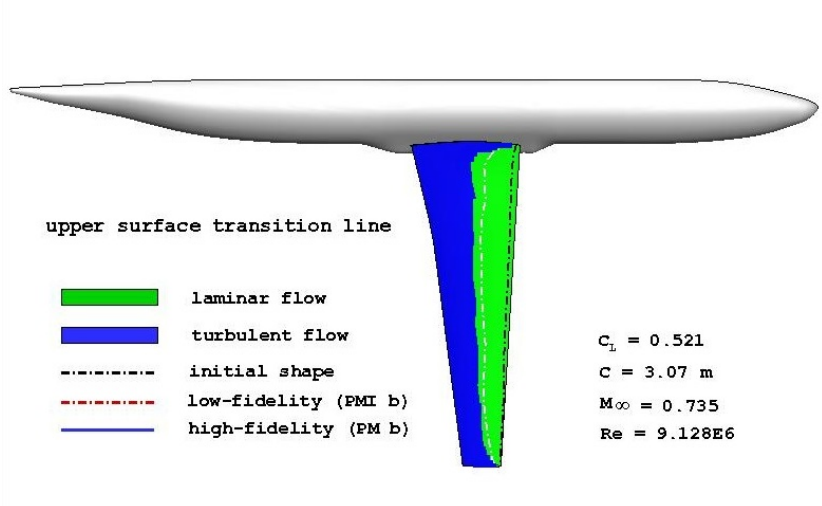

Figure 11. Transition lines on the upper surface of the baseline and optimized wing shape corresponding to *PMIb* and *PMb*.

 doi:10.20944/preprints202409.0973.v1

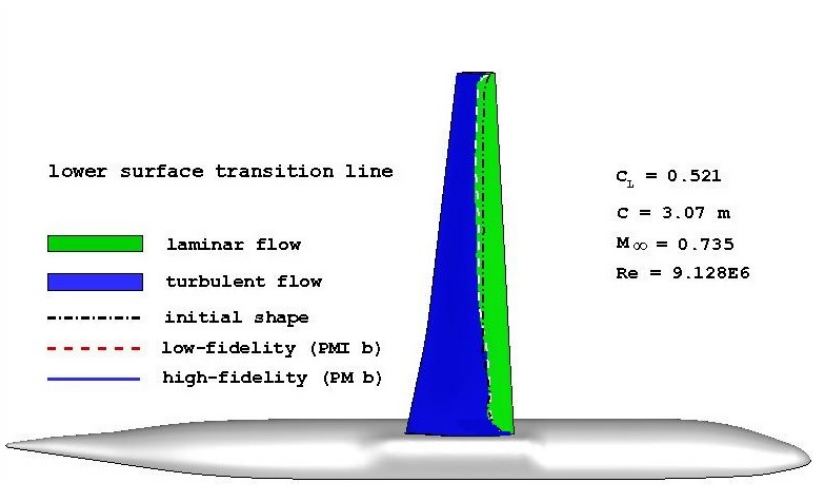

Figure 12. Transition lines on the lower surface of the baseline and optimized wing shape corresponding to *PMIb* and *PMb*.

5. Conclusion and Perspectives

Considered as an innovative research, the laminarization technology offers the designer an approach to significantly improve the aerodynamic performances of an aircraft. Therefore, the laminarization strategy remains one of the most advanced and effective drag reduction technology in the future. This research oriented paper is focused on the NLF wing design of a civil aircraft operating at transonic regimes, and includes the following subsections:

1) considering the aerodynamic performances of an optimized transonic laminar wing at high Reynolds number, it is found that the NLF wing needs to maintain a strong and long range of favorable pressure gradient on the wing surface, which induces a strong shock wave due to pressure recovery at the trailing edge. Therefore, it is necessary to control simultaneously both the laminar region on the surface of the wing and the shock intensity. Associated to the problem of NLF wing design, the design optimization of a laminar flow wing is solved by a multi-objective optimization problem maximizing laminar flow region and minimizing the shock wave intensity simultaneously; then a transonic NLF wing/airfoil design optimization model is numerically implemented and run effectively. Nearly 40% of the laminar flow area on the wing surface is achieved at the Reynolds number of 10^7.
2) a hierarchical evolutionary optimization design method using a variable-fidelity model is introduced, and a two-objective optimization design of transonic NLF wing is carried out. The analysis of the optimization results show that a hierarchical variable-fidelity model based optimization method in this paper can solve and provide to the designer an optimal set of Pareto solutions to the problem. These results confirm that a variable-fidelity model based hierarchical optimization method is feasible and effective.
3) many new techniques are introduced into the traditional variable fidelity optimization methods in this paper, such as search space contraction, reducing the number of design variables as well as population size reduction. Numerical experiments show that the hierarchical evolutionary optimization method combined with variable fidelity analysis, search space contraction and population size reduction can improve the optimization efficiency by nearly ten times, which further shows the potential of this method in solving practical complex engineering optimization problems.
4) optimized results of this paper achieved on the laminarization of 3D wings have been obtained with a cooperative Pareto game-GAs optimizer approach. Other strategies like Nash or Stackelberg games can provide also efficient solutions to the designer according to the physics of the

 doi:10.20944/preprints202409.0973.v1

problem, they are investigated for efficiency and quality comparison on 3D aircraft configurations. Due to large CPU-time computations requested for multi-objective optimization of wings, the design optimization of NLF 3D complete aircraft configurations remains still a challenge in the future that will necessitate combining large HPC facilities and artificial intelligence tools (machine learning, big data analysis, et al.).

Author Contributions: Data curation, S.L. and Y.C.; formal analysis, Z.T. and S.L.; funding acquisition, Z.T.; investigation, S.L. and Y.C.; methodology, S.L., Y.C. and Z.T.; project administration, Z.T.; resources, S.L. and Y.C.; software, S.L. and Y.C.; supervision, Z.T.; validation, S.L. and Y.C.; writing—original draft, S.L.; writing—review and editing, Z.T. and Y.C.; All authors have read and agreed to the published version of the manuscript.

Funding: This research was funded by the National Natural Science Foundation of China (12032011, 11772154), the Project Funded by the Priority Academic Program Development of Jiangsu Higher Education Institutions (PAPD).

Data Availability Statement: The datasets generated and analyzed during the current study are available from the corresponding author on reasonable request.

Conflicts of Interest: The authors declare no conflicts of interest.

References

1. Green, J. E. (2008). Laminar flow control-back to future. *38th fluid dynamics conference and exhibit*, Seattle, Washington.
2. Lee, J. D., & Jameson, A. (2009). Natural-laminar-flow airfoil and wing design by adjoint method and automatic transition prediction. *47th AIAA Aerospace sciences meeting*, Orlando, Florida, pp 1-25.
3. Amoignon, O. G., Pralits, J. O., Hanifi, A., Berggren, M., & Henningson, D. (2006). Shape optimization for delay of laminar-turbulent transition. *AIAA Journal*, *44*(5), 1009-1024.
4. Hua, J., Zhang, Z., Qiao, Z., & Wang, P. (1990). A transonic airfoil design method and example. *Acta Aerodynamic Sinica*, *8*(2), 117-123.
5. Song, W., Zhu, Z., Zhang, K., & Hang, Z. (2015). Simulations of the viscous flow around swept wings and optimization design using the RANS solver with automatic transition prediction. *Aerospace Science & Technology*, *26*(11), 23-29.
6. Zhang, Y. F., Fang, X. M., Chen, H. X., Fu, S., Duan, Z. Y., & Zhang Y. J. (2015). Supercritical natural laminar flow airfoil optimization for regional aircraft wing design. *Aerosp. Sci. Technol.*, *43*, 152-164. https://doi.org/10.1016/j.ast.2015.02.024.
7. Smith, A. M. O. (1956). *Transition, pressure gradient, and stability theory*, Douglas Aircraft Company.
8. Ingen, J. V., & Marios, K. (2011). A two-parameter method for eN transition prediction. *6th AIAA theoretical fluid mechanics conference*, Hawaii.
9. Arnal, D., Casalis, G., & Juillen, J. C. (1990). Experimental and theoretical analysis of natural transition on infinite swept wing. In: Arnal D., & Michel R. (eds). *Laminar-Turbulent Transition. International Union of Theoretical and Applied Mechanics*. Springer, Berlin.
10. Cebeci, T., & Stewartson, K. (2012). On stability and transition in three dimensional flows. *AIAA Journal*, *18*(4), 398-405.
11. Stock, H. W., & Haase, W. (2012). Feasibility study of eN transition prediction in Navier-Stokes methods for airfoils. *AIAA Journal*, *37*(10), 1187-1196.
12. Krumbein, A. (2008). eN transition prediction for 3D wing configuration using database methods and local, linear stability code. *Aerospace Science and Technology*, *12*(8), 592-598.
13. Song, W., Wu, M., Zhu, Z., Wu, T., Nie, H., Fan, T., & Han, Z. (2018). Transition prediction methods towards significant drag reduction via laminar flow technology. *Acta Aerodynamica Sinica*, *36*(2), 213-228.
14. Syberfeldt, A., & Rogstrom, J. (2018). A two-step multi-objectivization method for improved evolutionary optimization of industrial problems. *Appl. Soft Comput.*, *64*, 331-340. http://s.dic.cool/S/g881Qkw0.
15. Han, Z., Xu, C., Zhang, L., Zhang, Y., Zhang, K., & Song, W. (2020). Efficient aerodynamic shape optimization using variable-fidelity surrogate models and multilevel computational grids. *Chinese Journal of Aeronautics*, *33*(1), 31-47.
16. Huang, L., Gao, Z., & Zhang, D. (2013). Research on multi-fidelity aerodynamic optimization methods. *Chinese Journal of Aeronautics*, *26*(2), 279-286.

17. Gano, S. E., Renaud, J. E., & Sanders, B. (2005). Hybrid variable fidelity optimization by using a kriging - based scaling function. *AIAA Journal*, *43*(11), 2422-2450.
18. Tang, Z., Chen, Y., Zhang, L., & Periaux, J. (2019). Solving the two objective evolutionary shape optimization of a natural laminar airfoil and shock control bump with game strategies. *Archives of Computational Methods in Engineering*, *26*, 119-141.
19. Tang, Z., Chen, Y., Zhang, L. (2017) Natural laminar flow shape optimization in transonic regime with competitive Nash game strategy, *Applied Mathematical Modelling*, 48 (2017) 534-547.
20. Qin, N., Periaux, J., & Bugeda, G. (2020). *Advances in effective flow separation control for aircraft drag reduction: modeling, simulations and experimentations*, Springer.
21. Nubler, K., Lutz, T., Kramer, E., Colliss, S., & Babinsky, H. (2012). Shock control bump robustness enhancement. *50th AIAA Aerospace Science Meeting including the New Horizons Forum and Aerospace Exposition*, Nashville, Tennessee.
22. Liebeck, R. H. (1978). Design of subsonic airfoils for high lift. *Journal of Aircraft*, *15*(9), 547-561.
23. Boyd, G., & James, A. (1985). Trailing edge device for an airfoil. US Patent No. 4542868.
24. Burdette, D. A., & Martins, J. R. (2018). Design of a transonic wing with an adaptive morphing trailing edge via aerostructural optimization. *Aerosp. Sci. Technol.*, *81*, 192-203. https://doi.org/10.1016/j.ast.2018.08.004.
25. Mazaheri, K., Kiani, K. C., Nejati, A., Zeinalpour, M., & Taheri, R. (2015). Optimization and analysis of shock wave/boundary layer interaction for drag reduction by Shock Control Bump. *Aerosp. Sci. Technol.*, *42*, 196-208. https://doi.org/10.1016/j.ast.2015.01.007.
26. Chen, Y., Tang, Z., & Sheng, J. (2018). Trailing edge device application for the wave drag reduction in NLF airfoil multi-objective optimization. *Journal of Nanjing University of Aeronautics and Astronautics*, *50*(4), 548-557.
27. Tang, Z., Luo, S., Chen, Y., Zhao, X., & Wu., P. (2022). Hierarchical variable fidelity evolutionary optimization methods and their applications in aerodynamic shape design. *Applied Soft Computing*, 114 (2022) 108135, https://doi.org/10.1016/j.asoc.2021.108135.
28. Nash, J. (1951). Non-cooperative games. *Annals of Mathematics*, *54*(2), 286-295.
29. Stackelberg, H. (1934). *Marktform and Gleichgewicht*. Springer-Verlag Berlin Heidelberg.
30. Schaffer, J. D. (1985). Multiple objective optimization with vector evaluated genetic algorithms. *Proceedings of the 1st International Conference on Genetic Algorithms*, Pittsburgh, PA.
31. Goldberg, D. E. (1989). *Genetic algorithms in search, optimization and machine learning*, Addison-Wesley Professional.
32. Xu, J. K., Fu, Z. Y., Bai, J. P., Zhang, Y., Duan, Z. Y., & Zhang, Y. J. (2018). Study of boundary layer transition on supercritical natural laminar flow wing at high Reynolds number through wind tunnel experiment. *Aerosp. Sci. Technol.*, *80*, 221-231. https://doi.org/10.1016/j.ast.2018.07.007.
33. Tang, Z., Zhang, M., Hu, X. (2022). Optimal shape design and transition uncertainty analysis of transonic axisymmetric natural laminar flow nacelle at high Reynolds number. *Aerosp. Sci. Technol.*, *121*, 107345. https://doi.org/10.1016/j.ast.2022.107345.